

Velocity Distributions and Correlations in Homogeneously Heated Granular Media

Sung Joon Moon*, M. D. Shattuck†, and J. B. Swift

Center for Nonlinear Dynamics and Department of Physics, The University of Texas at Austin, Austin, TX 78712
(December 2, 2024)

We compare the steady state velocity distributions from our three-dimensional inelastic hard sphere molecular dynamics simulation for homogeneously heated granular media, with the predictions of a mean field-type Enskog-Boltzmann equation for inelastic hard spheres [van Noije & Ernst, *Gran. Matt.* **1**, 57 (1998)]. Although we find qualitative agreement for all values of density and inelasticity, the quantitative disagreement approaches $\sim 40\%$ at high inelasticity or density. By contrast the predictions of the pseudo-Maxwell molecule model [Carrillo, Cercignani & Gamba, *Phys. Rev. E*, **62**, 7700 (2000)] are both qualitatively and quantitatively different from those of our simulation. We also measure short-range and long-range velocity correlations exhibiting non-zero correlations at contact before the collision, and being consistent with a slow algebraic decay over a decade in the unit of the diameter of the particle, proportional to $r^{-(1+\alpha)}$, where $0.2 < \alpha < 0.3$. The existence of these correlations imply the failure of the molecular chaos assumption and the mean field approximation, which are responsible for the quantitative disagreement of the inelastic hard sphere kinetic theory.

I. INTRODUCTION

Granular materials are collections of noncohesive macroscopic dissipative particles and are encountered in nature and in the industry [1]. These materials exhibit a wide variety of phenomena depending on the external forcing. The rapid granular flow regime, where the collisions are modeled as instantaneous binary inelastic collisions, is reminiscent of a gas of hard spheres. Thus, a common theoretical approach for this regime is to model the system by means of the kinetic and the continuum equations for smooth inelastic hard spheres with the assumption of a velocity-independent coefficient of restitution [2]. In the kinetic theory approach, the mean field-type Boltzmann or Enskog-Boltzmann equation for inelastic hard spheres is used, and most techniques are directly transposed from the kinetic theory of a gas of elastic hard spheres [3]. It is known that this formulation is a good description for nearly elastic ($1 - e^2 \ll 1$, where e is the normal coefficient of restitution), and dilute cases. However, these theoretical models include approximations such as the truncation of series expansion or hierarchy, and the introduction of equation closure. The dissipative nature of the collision modifies the physics in a nontrivial way, and the accuracy and the limitation of the mean field-type kinetic description with these approximations for more inelastic, and more dense system is not yet well known. The extension of the theory for the more inelastic and dense case, including surface friction, is one of major goals of the current inelastic kinetic theory [4].

There is an attractor in the phase space of the granular media, because inelastic collisions dissipate kinetic energy. In the absence of an external energy source, a granular medium loses its kinetic energy through collisions and becomes a static pile. Thus, to reach a steady

state or an oscillatory state, a granular system requires an external energy source. In this paper, we investigate the steady state velocity distributions and velocity correlations of homogeneously heated granular media subject to a volumetric Gaussian white noise forcing. This system has been studied by several authors [5,6,12,18] as a reference system for the kinetic theory of granular media. In this system, particles collide inelastically, and execute Brownian motion between collisions. The motion is analogous to Brownian dynamics of hard sphere suspension, but here the kinetic energy is dissipated due to the inelastic collisions rather than hydrodynamic drag. This system is far from equilibrium, and the steady state velocity distribution deviates from the Maxwell-Boltzmann distribution. The distribution of homogeneously heated granular media was first theoretically studied by van Noije *et al.* [5], who obtained the approximate solutions to the inelastic hard sphere Enskog-Boltzmann equation with a Gaussian white noise forcing. In their study, the Sonine polynomial expansion method was used to construct the solution to the equation, and the series was truncated at the first nonvanishing term by assuming that the coefficient of the expansion converges rapidly as it does in the kinetic theory for elastic hard spheres. These results were tested against the Direct Simulation Monte Carlo (DSMC) method [6] of the inelastic Enskog-Boltzmann equation, and a good agreement was found, which confirmed the accuracy of the approximate analysis. However, the validity of the DSMC method relies on the validity of the inelastic (Enskog-)Boltzmann equation [7]. In the current study, we use a large molecular dynamics (MD) simulation (using up to 477,500 particles) of inelastic hard spheres to measure the steady state velocity distributions, and quantitatively examine the accuracy of the inelastic Enskog-Boltzmann equation model for this system. Our method is not restricted by the assumptions

used in the inelastic kinetic theory, and it has an advantage that correlations can develop but has a disadvantage that it may have a finite simulation size effect.

We also compare our results with theoretical predictions of Carrillo *et al.* [8], who obtained the steady state velocity distribution by using the pseudo-Maxwell molecule model [9]. The Maxwell molecule model is the special case of the inverse power law model for the inter-particle potential, whose potential has the form of $V(r) \sim r^{-4}$, where r is the inter-particle distance. This model has been widely used for analytical studies as a reference system for more realistic systems, because the model facilitates calculations involving linearized Boltzmann operator. The pseudo-Maxwell molecule model is an inelastic analog of the Maxwell molecule model.

The remainder of the paper is organized as follows. Section II presents the method of the numerical simulation, and Section III briefly reviews the theoretical results of the inelastic hard sphere model and the pseudo-Maxwell molecule model. In Section IV, simulation results of the velocity distributions are presented, and these are compared with the results of the theoretical predictions. The simulation results of the velocity correlations are also presented in this Section. The paper is summarized and concluded in Section V.

II. NUMERICAL SIMULATION

We simulate an ensemble of inelastic hard sphere particles of diameter σ in a three-dimensional (3d) cubic box of each side 105.3σ , which are subject to a volumetric Gaussian white noise forcing. Particles obtain the kinetic energy from the white noise forcing, execute Brownian motion in between collisions, and dissipate the kinetic energy through inelastic collisions. We assume that the dissipation due to the collision is characterized only by the normal coefficient of restitution e . To be consistent with the theoretical studies presented in Section III, we assume the normal coefficient of restitution does not depend on the relative velocity of colliding particles, and we neglect the rotational degrees of freedom. We use an event-driven MD code originally developed to simulate the patterns in vertically oscillated granular layers. Excellent agreement was found between simulations and experiments [10]. We modify this code to implement the Gaussian white noise forcing in between collisions. Brownian dynamics for hard sphere simulation was originated in the work of Ermak *et al.* [11], and the granular analog was introduced by Williams *et al.* [12] for their study of a one-dimensional system.

To implement Gaussian white noise forcing in an MD simulation, we start from a stochastic equation of motion for a particle. The equation of motion is given by

$$\ddot{x}_i(t) = \mathcal{F}_i^{(c)}(t) + \Gamma_i(t), \quad (1)$$

where the mass of the particle is unity, x_i is the i^{th} cartesian component of the position, $\mathcal{F}_i^{(c)}$ is the i^{th} component of the forcing due to the collisions, and $\Gamma_i(t)$ is the i^{th} component of the stochastic forcing. The stochastic forcing term satisfies

$$\langle \Gamma_i(t) \rangle = 0, \quad (2)$$

which assures that the fluctuation cancels out on the average, where $\langle \rangle$ is an ensemble average, and

$$\langle \Gamma_i(t)\Gamma_j(t') \rangle = 2F\delta_{ij}\delta(t-t'), \quad (3)$$

where F is the strength of the correlation, δ_{ij} is the Kronecker delta, and $\delta(t)$ is the delta function. Eq.(3) assures that the collisions well separated in time are statistically independent. We assume that all higher-order moments of the random variable $\Gamma_i(t)$ can be expressed in terms of the second moment, which is identical to the assumption that $\Gamma_i(t)$ is distributed according to the Gaussian distribution [13]. We implement an equation equivalent to Eq.(1) for a specific particle with a discrete time interval of a fixed value. It can be shown that the discrete Langevin equation for a Gaussian white noise for the velocity in between collisions is given by

$$v_i(t + \delta t) = v_i(t) + \sqrt{F}\sqrt{\delta t}G(0,1), \quad (4)$$

where F is the same quantity as in Eq.(3), δt is the time interval between the white noise forcing, and $G(0,1)$ is the unit Gaussian distribution random variable.

In the simulation, N_k particles are randomly chosen at every δt and are kicked in accordance with Eq.(4). To avoid the development of a mean flow in the system, particles to be kicked are randomly picked pairwise, and particles of this pair are kicked in opposite directions with the same speed to conserve the momentum. In an event-driven simulation, the random kickings are computationally expensive discrete events, because the collision list needs to be updated at each kicking. For the efficiency of the simulation, the mean kicking frequency needs to be minimized, or the mean kicking time for each particle $\bar{\delta t}$ ($= \delta t \cdot N/N_k$) needs to be maximized, where N is the total number of particles. We empirically checked in the simulation that the velocity distributions do not change if $\bar{\delta t}$ is less than $1/(5\nu_{coll})$, where ν_{coll} is the mean collision frequency. We also checked that the velocity distributions do not depend on the choice of N_k and δt in these cases. Thus we keep $\bar{\delta t} \sim 1/(10\nu_{coll})$ throughout the simulations. The volume fraction ν varies from ν_o ($= 4.29\%$) to $5\nu_o$ ($= 21.4\%$), which corresponds to 95,495 to 477,500 in the number of particles. Since the collisions are instantaneous, there is only one time scale determined by the granular temperature, σ/\sqrt{T} , where T is defined in Eq.(6). Therefore the temperature only rescales the time, and the results are expected to be independent of T . However, we fix the granular temperature at approximately the same value throughout the simulations. We prepare the initial conditions by locating particles in a regular lattice. We heat them, and wait

until the transients decay away, ensuring that a steady state is reached. The data are taken periodically with a fixed time interval Δt . To assure that each data set is statistically uncorrelated, Δt is chosen larger than $5/\nu_{coll}$ in all cases, and $\Delta t \sim 10/\nu_{coll}$ in most cases. We obtain 50 such data sets for each simulation, and the error bars shown in this paper are the standard deviations of these data sets. A periodic boundary condition is imposed in all direction.

III. REVIEW OF THEORY

In this Section, we briefly review the results of the previous theoretical studies of van Noije *et al.* [5] and of Carrillo *et al.* [8]. Both studies are based on the inelastic Enskog-Boltzmann equation.

Following standard procedures of the kinetic theory, it can be shown that the inelastic Enskog-Boltzmann equation for homogeneous granular particles with a white noise forcing is given by

$$\frac{\partial f}{\partial t} = Q(f, f) + L_{FP}f, \quad (5)$$

where $f = f(\mathbf{c}, t)$ is the single particle distribution function, $Q(f, f)$ is the collision operator, $\mathbf{c} = \mathbf{v}/\sqrt{2T(t)}$ is the velocity scaled by the characteristic velocity, and the mass is unity. $T(t)$ is the granular temperature, defined as the variance of the velocity distribution per degree of freedom. For a three-dimensional system,

$$T(t) = \frac{1}{3} \langle |\mathbf{v}(t) - \langle \mathbf{v}(t) \rangle|^2 \rangle. \quad (6)$$

The Fokker-Planck operator L_{FP} is a diffusion operator in the velocity space, which is given by

$$L_{FP} = F \nabla_{\mathbf{c}}^2, \quad (7)$$

where F is the strength of the correlation of Gaussian white noise stochastic forcing, and $\nabla_{\mathbf{c}}^2$ is the Laplacian in the velocity space. The collision operator, $Q(f, f)$, is chosen according to the inter-particle potential model, and the most obvious choice for the granular particles is the inelastic hard sphere collision operator.

Van Noije *et al.* [5] obtained the steady state solutions to Eq.(5) using the inelastic hard sphere collision operator, and Carrillo *et al.* [8] obtained the steady state solutions to Eq.(5) using the pseudo-Maxwell collision operator. In both analyses, the Sonine polynomial expansion method was used to construct the solution to the inelastic Enskog-Boltzmann equation. Sonine polynomials are associated Laguerre polynomials and have been used to construct solutions to the Boltzmann equation since Burnett [14] introduced them in the study of nonuniform gases. They are exact eigenfunctions of the linearized

Boltzmann equation for Maxwell molecules. This expansion also leads to rapidly converging solutions of the linearized Boltzmann equation for other short-range repulsive potentials [3]. The definition of Sonine polynomials of lower parameter 1/2 is given by

$$S_{1/2}^{(n)}(x) = \sum_{p=0}^n \frac{(\frac{1}{2} + n)!}{(\frac{1}{2} + p)!(n - p)!p!} (-x)^p. \quad (8)$$

In the current study, c^2 is the argument of Sonine polynomials. The orthogonality relation with this argument is

$$\int_0^\infty c^2 e^{-c^2} S_{1/2}^{(n)}(c^2) S_{1/2}^{(m)}(c^2) dc = \frac{1}{2} \delta_{nm} \frac{(\frac{1}{2} + n)!}{n!}. \quad (9)$$

The first three Sonine polynomials are given by

$$\begin{aligned} S_{1/2}^{(0)}(c^2) &= 1, \\ S_{1/2}^{(1)}(c^2) &= \frac{3}{2} - c^2, \\ S_{1/2}^{(2)}(c^2) &= \frac{15}{8} - \frac{5}{2}c^2 + \frac{1}{2}c^4. \end{aligned}$$

For the inelastic hard sphere model, van Noije *et al.* [5] obtained the steady state solutions for 2d and 3d cases, by using the moment method [15] which was used in the analysis of the velocity distributions of homogeneously cooling of a freely evolving system. They expand the solution in Sonine polynomials and neglect terms of higher order than the first nonvanishing correction to the Maxwell-Boltzmann distribution. The steady state solution for the 3d case, $f^s(c)$, is obtained as

$$f^s(c) = f_{MB}(c)[1 + a_2^{HS} S_{1/2}^{(2)}(c^2)], \quad (10)$$

where

$$f_{MB}(c) = \frac{4}{\sqrt{\pi}} c^2 \exp(-c^2) \quad (11)$$

is the Maxwell-Boltzmann distribution (multiplied by an integration factor), and

$$a_2^{HS}(d, e) = \frac{16(1 - e^2)(1 - 2e^2)}{73 + 56d - 24ed - 105e + 30(1 - e)e^2}, \quad (12)$$

where d is the dimensionality of the system ($d = 3$ in the current study).

For the pseudo-Maxwell molecule model, Carrillo *et al.* [8] obtained the steady state solution to Eq.(5) by doubly expanding the solution in the energy dissipation rate, $\epsilon = (1 - e^2)/4$, and in Sonine polynomials. The deviation from the Maxwell-Boltzmann distribution was obtained up to the order of ϵ^4 [16]. The solution with the first nonvanishing correction to the Maxwell-Boltzmann distribution is of the order of ϵ^2 , which is given by

$$f^s(c) = f_{MB}(c)[1 + \epsilon^2 \cdot 4S_{1/2}^{(2)}(c^2)], \quad (13)$$

The first order deviations from the Maxwell-Boltzmann distribution in the two models have the same basis function $S_{1/2}^{(2)}(c^2)$, the second Sonine polynomial. For the sake of comparison, we rewrite the normalized deviations from the Maxwell-Boltzmann in the two models as follows,

$$g^{HS}(e, c) = \frac{\Delta f^{HS}(e, c)}{f_{MB}(c)} = a_2^{HS}(e) S_{1/2}^{(2)}(c^2), \quad (14)$$

$$g^{MM}(e, c) = \frac{\Delta f^{MM}(e, c)}{f_{MB}(c)} = a_2^{MM}(e) S_{1/2}^{(2)}(c^2), \quad (15)$$

where

$$a_2^{MM}(e) = (1 - e^2)^2/4 = 4e^2, \quad (16)$$

and *HS* and *MM* stands for inelastic hard spheres and pseudo-Maxwell molecules respectively. The coefficients of the second Sonine polynomial for the two models, $a_2^{HS}(e)$ and $a_2^{MM}(e)$, are compared in Figure 1.

To summarize, the results of the inelastic hard sphere model and those of the pseudo-Maxwell molecule model are different mainly in two ways:

(1) In the inelastic hard sphere model, there is a crossover from positive to negative values in $a_2^{HS}(e)$ as e increases, and it is negative for $1/\sqrt{2} < e < 1.0$, whereas in the pseudo-Maxwell molecule model, $a_2^{MM}(e)$ is positive definite, $4e^2$. The high energy tail is always overpopulated in the pseudo-Maxwell molecule model, whereas it is underpopulated for $e > 1/\sqrt{2}$ in the inelastic hard sphere model.

(2) The deviation from the Maxwell-Boltzmann distribution in the pseudo-Maxwell molecule model is quantitatively much larger than that in the inelastic hard sphere model. Note that the analysis of the pseudo-Maxwell molecule model analysis has a small inelasticity assumption, whereas the analysis of the inelastic hard sphere model has no such assumption.

IV. SIMULATION RESULTS

A. velocity distributions

We measure the velocity of each particle periodically in time with a fixed time interval of $\Delta t \sim 10/\nu_{coll}$. The time interval Δt is chosen to assure that each data set is statistically uncorrelated. The measured velocities are binned, and the bin size is $\Delta c = 0.1$. Figure 2 shows the velocity distributions for two coefficients of restitution, $e = 0.1$ and $e = 0.9$, obtained in the simulation. As in the inelastic hard sphere theory, high velocity tail is overpopulated for $e = 0.1$, and slightly underpopulated for $e = 0.9$, compared to the Maxwell-Boltzmann distribution (thick solid line).

We define the deviation from the Maxwell-Boltzmann distribution, $g(c)$, in the following relation,

$$f^s(c) = f_{MB}(c)[1 + g(c)]. \quad (17)$$

Assuming $g(c)$ is a smooth function in the small interval $c_o < c < c_o + \Delta c$, $g(c)$ can be approximated as

$$g(c_o + \frac{\Delta c}{2}) \approx \frac{\int_{c_o}^{c_o + \Delta c} f^s(c) dc}{\int_{c_o}^{c_o + \Delta c} \frac{4}{\sqrt{\pi}} e^{-c^2} c^2 dc} - 1. \quad (18)$$

In Eq.(18), the numerator is the total number of particles in the bin, which is a number counted in the simulation, and the denominator can be evaluated using the error function table. Figure 3 shows $g(c)$ calculated using Eq.(18) for the data in Figure 2. For direct comparison between our simulation results and the above theoretical predictions, we calculate the coefficient of the second Sonine polynomial, a_2 , from our measurements. As in the theoretical studies, we assume $f^s(c)$ is expanded in Sonine polynomials,

$$f^s(c) = f_{MB}(c)[1 + \sum_{k=2}^{\infty} a_k S_{1/2}^{(k)}(c^2)], \quad (19)$$

where a_1 is not included, because it is identically zero in theory. We checked in the simulation a_1 is less than 10^{-4} in all cases. In the simulation, we can use either of the following two formulae to calculate a_k , the coefficient of the k^{th} Sonine polynomial. Firstly, a_k 's can be obtained from the following numerical integration, using the orthogonality relation of Sonine polynomials,

$$a_k = \frac{2^k k!}{(2k+1)!!} \int_0^{\infty} f^s(c) S_{1/2}^{(k)}(c^2) dc. \quad (20)$$

Secondly, we can make use of the recurrence relation of a_k 's. Starting from the definition of Sonine polynomials, Eq.(8), it can be shown that for $k > 2$, a_k satisfies

$$a_k = \frac{(-1)^k 2^k}{(2k+1)!!} < c^{2k} > + (-1)^{k+1} + \sum_{p=1}^{k-2} (-1)^{p+1} \binom{k}{p} a_{k-p}, \quad (21)$$

where $< c^{2k} >$ is the $2k^{th}$ moment. It is straightforward to numerically evaluate the integration in both formula. The above two relations, Eq.(20) and Eq.(21), are mathematically identical. However, the errors of the lower k coefficients are accumulated on higher k coefficients in Eq.(21), whereas each a_k is determined independently in Eq.(20). The results obtained using Eq.(20) and Eq.(21) are nearly the same for small k , and they deviate more for larger k . Figure 4 shows a_2 obtained using Eq.(20), a_2^{MD} , which are compared with the theoretical results Eq.(12), a_2^{HS} , and Eq.(16), a_2^{MM} . The simulation results deviate more from the predictions of the inelastic hard sphere kinetic theory as the system becomes more inelastic. Figure 4 shows a_2^{MD} has a crossover between the positive and the negative values at around $e \sim 0.8$. The pseudo-Maxwell molecule model does not predict this crossover

behavior of a_2 , and the results of this model deviate quantitatively from the kinetic theory and simulations of the inelastic hard sphere model.

In the simulation, all a_k 's can be obtained by using Eq.(20), in principle. For larger k , the weight of the high velocity data exhibiting strong fluctuations become larger, and so does the uncertainty of a_k . We calculate up to a_5 for various coefficients of restitution from the simulation, and these are shown in Figure 5. In Figure 5, for nearly elastic case, $e = 0.9$, the series converges rapidly as in many cases of elastic hard spheres. However, as the system becomes more inelastic, the series converges more slowly. For $e = 0.1$, a_4 is about 30% of a_2 . In Figure 6, we show how the first few nonvanishing coefficients of the Sonine polynomial series obtained in the simulation affect the fitting. Open circles are measured data from the simulation, and the error bars are not included for better comparison with fitting curves. The simulation results are fitted by successively including up to a_2, a_3 , and a_4 obtained in the simulation, which are shown as three curves. For $e = 0.1$, a_2 fits the measured data well up to $v \sim 3\sqrt{2T} \sim 5T$, but the high tail is fitted well only when the series keeps up to a_4 . For $e = 0.9$, it shows the same qualitative tendency. When we fit the data only with a_2 in this case, $f^s(c)$ is negative for $c > 4.1$ and becomes negative infinity as c goes to infinity. Such nonphysical behavior disappears when we include a_3 .

In the theoretical predictions, the steady state velocity distribution, or a_2 , does not depend on the density, and it is a function of the coefficient of restitution and the dimensionality only. However, in our simulation, we find that it also depends on the density. Figure 7 shows the density dependence of a_2 , which are compared with the theoretical predictions (thick dashed lines). The value of a_2 decreases as the system becomes more dilute. For the smallest volume fraction we used, ν_o , the value of a_2 deviates by only few percent from the predictions of the inelastic hard sphere theory. As shown in Figure 5, a_3 's are very small. We plot a_4 's for various densities in Figure 8. It follows the same tendency as a_2 does; as the system becomes more dense, a_4 gets larger. Error bars for these data are bigger than those for a_2 , because in calculating a_4 , higher velocity data have more weight, which exhibits stronger fluctuations.

Finally, we examine the asymptotic behavior of the high energy tails of the velocity distribution functions. Van Noije *et al.* [5] found for this system a high energy tail $\tilde{f}(c) \sim \exp(-\mathcal{A}'c^{3/2})$. We measure the velocity distribution function in x -direction $f_x(c_x)$, where

$$\begin{aligned} 1 &= \int \tilde{f}(c) d\mathbf{c} \\ &= \int \int \int f_x(c_x) f_y(c_y) f_z(c_z) dc_x dc_y dc_z, \end{aligned} \quad (22)$$

and $c_x = v_x/\sqrt{2T}$, and so on. To investigate the power of the argument of the exponential function, we renormalize

$f_x(c_x)$ with its maximum value, and plot it for various coefficients of restitution in Figure 9. We observe the crossover behavior from $\sim \exp(-\mathcal{A}c^2)$ to $\sim \exp(-\mathcal{A}'c^{3/2})$ as c increases, for $e \leq 0.5$.

B. Velocity correlations

Two major approximations imposed in the kinetic theory discussed in Section III are the mean field approximation and the truncation of the hierarchy using the molecular chaos assumption. In this Section, we examine the validity of the above approximations for this system by quantitatively investigating the parallel velocity correlations, in long-range and short-range respectively. It is known that a system of granular media exhibits strong spatial correlations [12,17,18], such as velocity correlations, but there is still the lack of a quantitative study of a 3d system. We suggest that the deviation of a_2^{MD} from a_2^{HS} originates from the failure of the above approximations.

We define the parallel velocity correlation function as

$$\langle c_{1,\parallel} c_{2,\parallel} \rangle = \frac{1}{N} \int \langle \mathbf{c}(\mathbf{r} + \mathbf{r}') \cdot \hat{\mathbf{r}} \rho(\mathbf{r} + \mathbf{r}') \mathbf{c}(\mathbf{r}') \cdot \hat{\mathbf{r}} \rho(\mathbf{r}') \rangle d\mathbf{r}', \quad (23)$$

where $\hat{\mathbf{r}} = \mathbf{r}/|\mathbf{r}|$, and $\rho(\mathbf{r})$ is the local particle density,

$$\rho(\mathbf{r}) = \sum_{i=1}^N \delta(\mathbf{r} - \mathbf{r}_i). \quad (24)$$

In the simulation, we approximately evaluate this quantity using the following formula,

$$\langle c_{1,\parallel} c_{2,\parallel} \rangle = \sum \frac{\mathbf{c}_{1,\parallel} \mathbf{c}_{2,\parallel}}{N_r}, \quad (25)$$

where the parallel direction is along the line of centers of the particle pair under consideration, N_r is the number of particles in a shell of thickness δr and inner radius r , and the summation is done over N_r . We use $\delta r = 0.1053\sigma$.

1. Long-range correlations

The parallel velocity correlations are also obtained by averaging over 50 statistically uncorrelated data sets. Figure 10 shows those for various coefficients of restitution at a fixed volume fraction, $5\nu_o$, as a function of dimensionless distance r/σ . Figure 11 shows those for various densities. The data are shown only for $r/\sigma < 30$, because they are subject to the finite system size effect for larger r/σ . The parallel velocity correlations are consistent with slow algebraic decay over a decade, $\sim r^{-(1+\delta)}$, where $0.2 < \delta < 0.3$. This behavior is close to the theoretical prediction of van Noije *et al.* [18], who predicted the r^{-1} power law from the mode coupling theory.

The velocity correlations in this system are consistent with algebraically decaying behavior, and these correlations get stronger for more inelastic or more dense system. It implies that the mean field approximation is reliable only for nearly elastic and dilute cases.

2. Short-range correlations

In this section, we investigate the velocity correlations at contact before the collision, to examine the validity of the molecular chaos assumption. A non-zero value of these correlations is the signature of the failure of the molecular chaos assumption. Since only the normal component of relative velocity of colliding particles are reduced at the collision, the velocities are more “parallelized” after the collision. If the velocities are already parallelized before the collision, it would indicate that the colliding pair have “memory” on the collisions in the past, and they are correlated. We find that for high inelasticity and density, the pre-collisional parallel velocity correlation value reaches up to $\sim 15\%$ of the temperature. Even for dilute or nearly elastic cases, these are not negligibly small.

We calculate the velocity correlations of pre- and post-collisional states by evaluating Eq.(25) only for approaching ($\mathbf{r}_{12} \cdot \mathbf{c}_{12} < 0$) and separating particles ($\mathbf{r}_{12} \cdot \mathbf{c}_{12} > 0$) respectively, where $\mathbf{x}_{12} = \mathbf{x}_1 - \mathbf{x}_2$ for $\mathbf{x} = \mathbf{r}$ or \mathbf{c} . Figure 12 shows the pre-collisional state of short-range ($1 < r/\sigma < 2$) parallel velocity correlations for various coefficients of restitution, and Figure 13 shows the post-collisional state of short-range parallel velocity correlations for various coefficients of restitution. The values of the pre-collisional correlations are not negligible compared to the temperature of the system. Post-collisional correlations are more than twice as large as pre-collisional correlations.

The maximum values of the velocity correlations in Figure 12 and in Figure 13 are not the values at the contact, $r = \sigma$, because of the finite size of the bins in the measurements, instead those are values at $r/\sigma = 1.053$. The values at $r = \sigma$ are estimated by extrapolating the data in the interval $1 < r/\sigma < 2$ using the least square fit with fifth-order polynomials. Figure 14 shows such parallel velocity correlations at $r = \sigma$ as a function of the coefficient of restitution, and Figure 15 shows them as a function of the density, as well as values at $r/\sigma = 1.053$. Since the velocity correlation changes rapidly as r/σ decreases to 1, these estimations may be only regarded as approximate lower bounds. There are no error bars for estimated values, because these are extrapolated values from the average values, and the error bars are not systematically determined. The error should be of the same order as the values at $r/\sigma = 1.053$. The velocity correlations at contact of this system show almost linear behavior both in density and the coefficient of restitution.

V. DISCUSSION

We have investigated the velocity distributions and parallel velocity correlations of 3d homogeneously heated granular media for various densities and inelasticities, using an inelastic hard sphere MD simulation. The deviations from the Maxwell-Boltzmann distribution in our simulations qualitatively agree with the results of the mean field-type inelastic hard sphere kinetic theory [5], but we found that there is systematic quantitative difference. We observe the high energy tails are consistent with $\sim \exp(-\mathcal{A}c^{3/2})$ for $e \leq 0.5$, but not for others. Since the elastic case ($e = 1.0$) has no crossover from $\sim \exp(-\mathcal{A}c^2)$ to $\sim \exp(-\mathcal{A}'c^{3/2})$, we expect that this crossover behavior may occur at higher velocities as e approaches to 1.0, if it occurs. However, we are not able to check whether the crossover occurs for $e > 0.5$ or never occurs, because our system is finite.

The steady state velocity distributions in the simulation depend on the density as well as the coefficient of restitution, whereas they depend only on the latter in the theory. The discrepancy between our simulation results and the theoretical predictions increases as the system becomes more inelastic or more dense, and the quantitative disagreement reaches up to $\sim 40\%$ for high inelasticity or density. This behavior is consistent with the results of van Noije *et al.* [18,19], who found that the collision frequency measured in a 2d MD simulation deviates more from the predictions of the inelastic Enskog-Boltzmann equation as the system becomes more inelastic. We suggest that the disagreement originates from the failure of two major approximations in the theory, the mean field approximation, and the molecular chaos assumption. To examine the accuracy and the limitation of these approximations, we quantitatively investigated the parallel velocity correlations of this system.

We found that the long-range parallel velocity correlations are consistent with a slow algebraic decay, $\sim r^{-(1+\delta)}$, where $0.2 < \delta < 0.3$. This result is close to the theoretical predictions of van Noije *et al.* [18], who renormalized various quantities such as the collision frequency using the mode coupling theory, and predicted r^{-1} power law for velocity correlations in homogeneously heated 3d granular media. Because of these strong correlations, the mean field approximation for granular media is not a good one unless the system is nearly elastic or very dilute.

We also found that the velocities are correlated at contact before the collision. We measured the short-range velocity correlations of pre- and post-collisional states separately to examine the validity of the molecular chaos assumption. The pre-collisional correlations at contact are about a half of the post-collisional correlations. The correlations at contact are almost linearly proportional to both the density and the coefficient of restitution, which is consistent with the recent results of Soto *et al.* [20],

who studied the velocity correlations of homogeneously cooling granular media in nearly elastic regime.

We also examined the convergence of the Sonine polynomial expansion technique used in the inelastic kinetic theory, and find that the series converges more slowly as the system becomes more inelastic. Finally, we compared the steady state velocity distributions in the simulations with the theoretical predictions of Carrillo *et al.* [8], who studied the inelastic Enskog-Boltzmann equation for pseudo-Maxwell molecule model. We found that the velocity distribution function predicted by the pseudo-Maxwell molecule model differ qualitatively from those predicted by the inelastic hard sphere model.

ACKNOWLEDGMENTS

The authors thank J. A. Carrillo, C. Bizon, A. Santo, I. Gamba, D. I. Goldman, W. D. McCormick and H. L. Swinney for helpful discussion. This work was supported by the Engineering Research Program of the Office of Basic Energy Sciences of the Department of Energy (Grant DE-FG03-93ER14312).

APPENDIX

A. Derivation of Eq. (18)

The deviation from the Maxwell-Boltzmann distribution, $g(c)$, is defined as in Eq.(17),

$$f^s(c) = f_{MB}(c)[1 + g(c)]. \quad (\text{A1})$$

In the simulation, we measure the number of particles in each bin,

$$\int_{c_o}^{c_o+\Delta c} f^s(c)dc = \int_{c_o}^{c_o+\Delta c} \frac{4}{\sqrt{\pi}} e^{-c^2} c^2 [1 + g(c)]dc, \quad (\text{A2})$$

where the bin is for $c_o < c < c_o + \Delta c$, and Δc is the bin size. It is possible to numerically solve for $g(c)$ from Eq.(A2), however, we get an approximate expression for $g(c)$ by assuming $g(c)$ is smooth and Δc is small enough;

$$\int_{c_o}^{c_o+\Delta c} e^{-c^2} c^2 g(c)dc \approx g(c_o + \frac{\Delta c}{2}) \int_{c_o}^{c_o+\Delta c} e^{-c^2} c^2 dc. \quad (\text{A3})$$

Eq.(A2) can be read

$$g(c_o + \frac{\Delta c}{2}) \approx \frac{\int_{c_o}^{c_o+\Delta c} f^s(c)dc}{\int_{c_o}^{c_o+\Delta c} \frac{4}{\sqrt{\pi}} e^{-c^2} c^2 dc} - 1. \quad (\text{A4})$$

B. Derivation of Eq. (21)

Starting from the definition of Sonine polynomials,

$$S_{1/2}^{(n)}(x) = \sum_{p=0}^n \frac{(\frac{1}{2} + n)!}{(\frac{1}{2} + p)!(n-p)!p!} (-x)^p, \quad (\text{B1})$$

it can be shown that

$$c^{2k} = \sum_{p=0}^k \frac{(-1)^{k+p} (\frac{1}{2} + k)! k!}{(\frac{1}{2} + k - p)! p!} S_{1/2}^{(k-p)}(c^2). \quad (\text{B2})$$

We assume the following Sonine polynomial expansion of the distribution function,

$$f^s(c) = f_{MB}(c)[1 + \sum_{p=2}^{\infty} a_p S_{1/2}^{(p)}(c^2)]. \quad (\text{B3})$$

Using Eq.(B2) and Eq.(B3), $2k^{th}$ moment reads

$$\langle c^{2k} \rangle = \frac{(2k+1)!!}{2^k} [1 + \sum_{p=0}^{k-2} (-1)^{k+p} \binom{k}{p} a_{k-p}], \quad (\text{B4})$$

or

$$a_k = \frac{(-1)^k 2^k}{(2k+1)!!} \langle c^{2k} \rangle + (-1)^{k+1} + \sum_{p=1}^{k-2} (-1)^{p+1} \binom{k}{p} a_{k-p}, \quad (\text{B5})$$

where $k > 2$.

* Electronic mail: moon@chaos.ph.utexas.edu

† Current address: Department of Physics, City College of CUNY, New York, NY 10031-9198

- [1] H. M. Jaeger, S. R. Nagel, and R. P. Behringer, *Rev. Mod. Phys.* **68**, 1259 (1996)
- [2] S. B. Savage and D. J. Jeffery, *J. Fluid Mech.* **110**, 255 (1981); P. K. Haff, *J. of Fluid Mech.* **134**, 401 (1983); J. T. Jenkins and S. B. Savage, *J. Fluid Mech.* **130**, 187 (1983); C. K. K. Lun, S. B. Savage, D. H. Heffery, and N. Chepurny, *J. Fluid Mech.* **140**, 223 (1984); J. T. Jenkins and M. W. Richman, *Arch. Ration. Mech. Anal.* **87**, 355 (1985)
- [3] S. Chapman and T. G. Cowling, *The Mathematical Theory of Non-uniform Gases*. Cambridge University Press, (1970)
- [4] I. Goldhirsh, *Chaos* **9**, 659 (1999)
- [5] T. P. C. van Noije and M. H. Ernst, *Gran. Matt.* **1**, 57 (1998)
- [6] J. M. Montanero and A. Santos, *Gran. Matt.* **2**, 53 (2000)
- [7] G. A. Bird *Molecular Gas Dynamics and the Direct Simulation of Gas Flows*. Oxford Science Publications, (1994)

- [8] J. A. Carrillo, C. Cercignani, and I. M. Gamba, Phys. Rev. E, **62**, 7700 (2000)
- [9] A. V. Bobylev and J. A. Carrillo and I. M. Gamba, J. Stat. Phys. **98**, 743 (2000)
- [10] C. Bizon, M. D. Shattuck, W. D. McCormick, and H. L. Swinney, Phys. Rev. Lett. **80**, 57 (1998)
- [11] D. L. Ermak and J. A. McCammon, J. Chem. Phys. **69**, 1352 (1978)
- [12] D. R. M. Williams and F. C. MacKintosh, Phys. Rev. E **54**, R9 (1996)
- [13] R. Balescu, *Equilibrium and Nonequilibrium Statistical Mechanics*. John Wiley & Sons, Inc. (1975)
- [14] D. Burnett, Proc. London Math. Soc. **2**, 39, 385 (1935)
- [15] A. Goldshtein and M. Shapiro, J. of Fluid Mech. **282**, 75 (1995)
- [16] J. A. Carrillo, private communication
- [17] M. R. Swift, M. Boamfa, S. J. Cornell, and A. Maritan, Phys. Rev. Lett. **80**, 4410 (1998); J. A. G. Orza, R. Brito, T. P. C. van Noije, and M. H. Ernst, Int. J. Mod. Phys. C **8**, 953 (1998)
- [18] T. P. C. van Noije, M. H. Ernst, E. Trizac, and I. Pagonabarraga, Phys. Rev. E, **59**, 4326 (1999)
- [19] E. Trizac, private communication
- [20] R. Soto and M. Mareshal, Phys. Rev. E **63**, 041303 (2001)

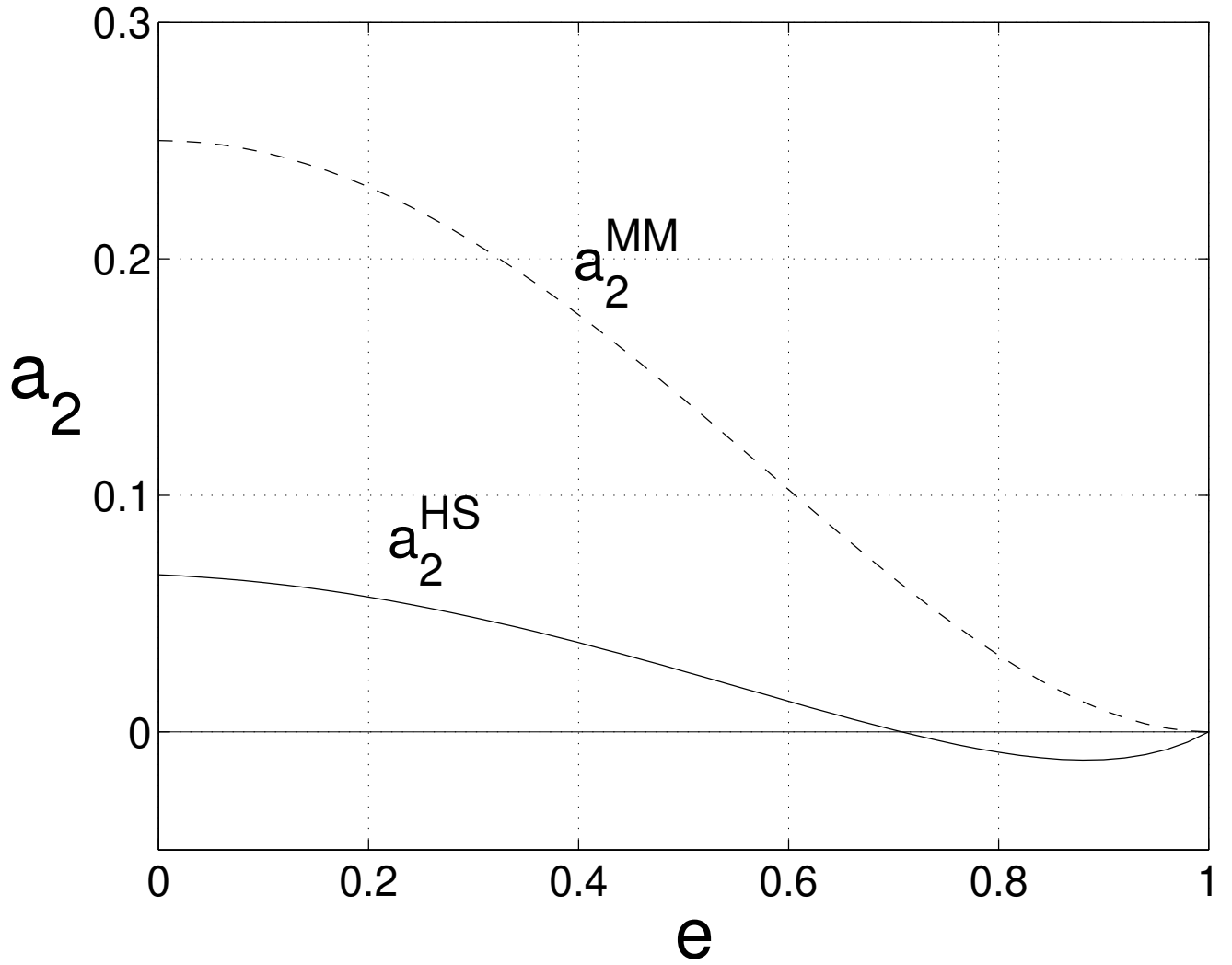


FIG. 1. The deviation from the Maxwell-Boltzmann distribution obtained in the theory, a_2 , as a function of the coefficient of restitution e . $a_2^{\text{HS}}(e)$ is the coefficient of the second Sonine polynomial for the inelastic hard sphere model, and $a_2^{\text{MM}}(e)$ is that for the pseudo-Maxwell molecule model.

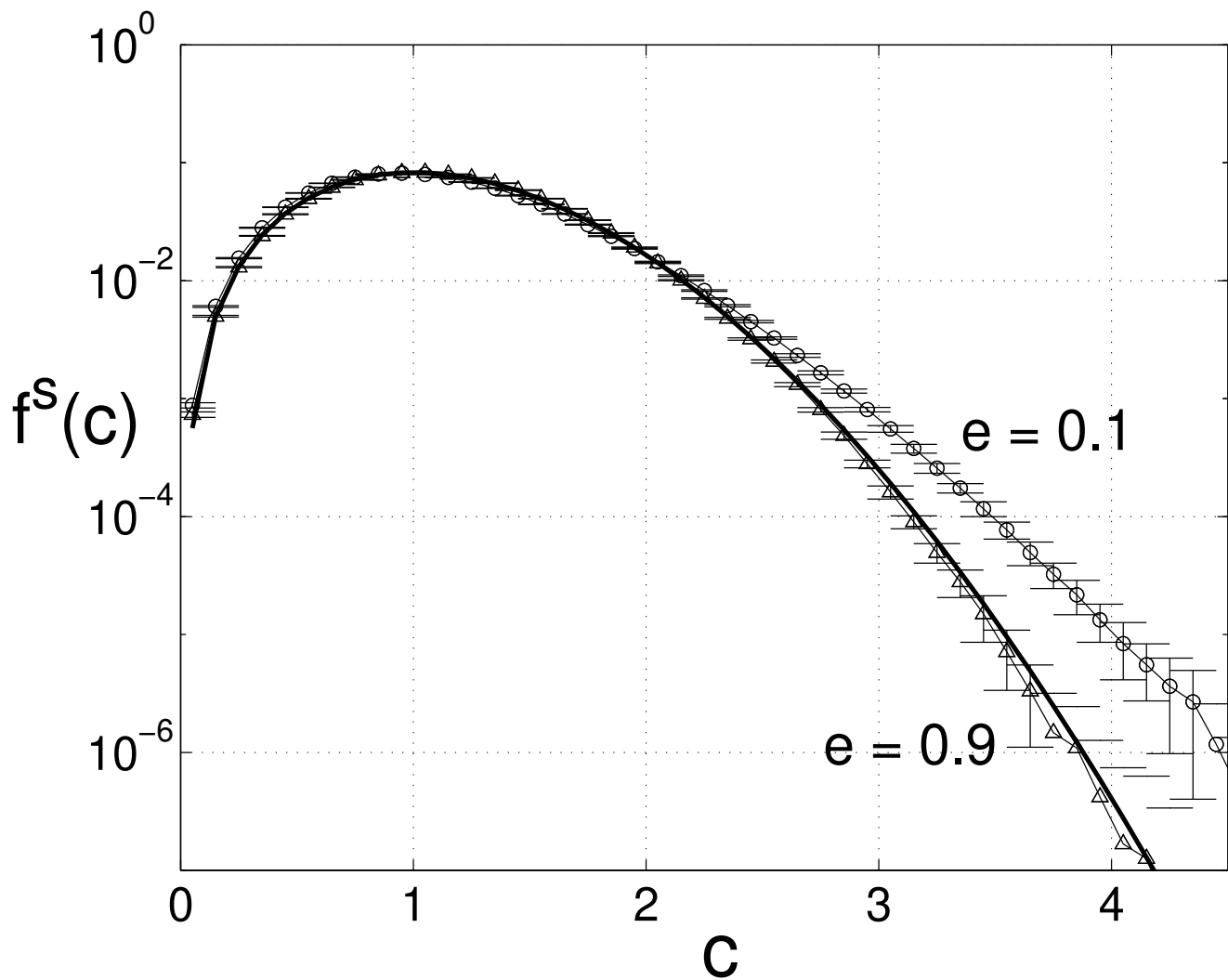


FIG. 2. The steady state velocity distributions, $f^s(c)$, obtained from the simulation for two coefficients of restitution, $e = 0.1$ and $e = 0.9$. The volume fraction is $5\nu_o$. The thick solid line is the Maxwell-Boltzmann distribution function.

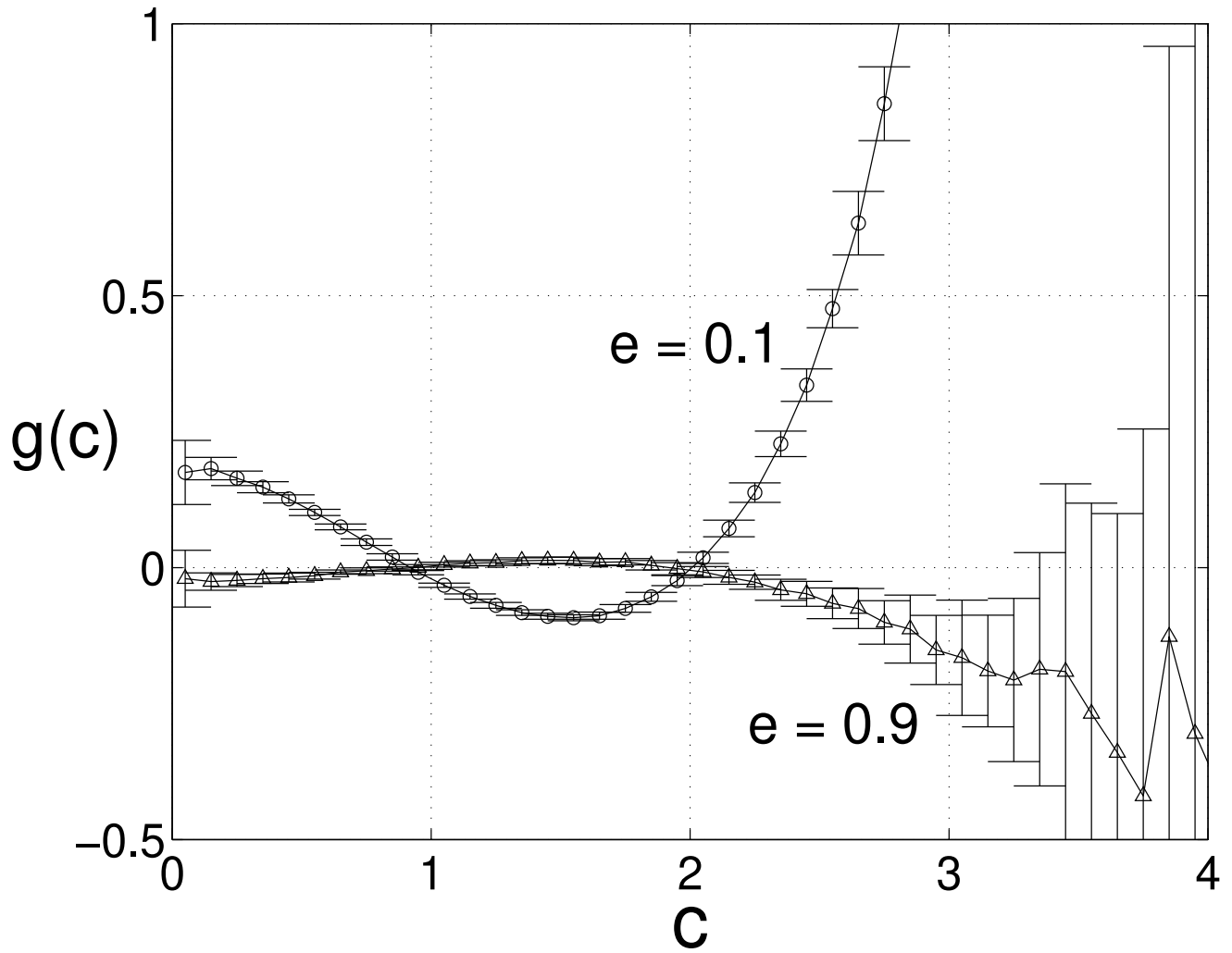


FIG. 3. The normalized deviation from the Maxwell-Boltzmann distribution, $g(c)$, obtained from the simulation for two coefficients of restitution, $e = 0.1$ and $e = 0.9$. The volume fraction is $5\nu_o$.

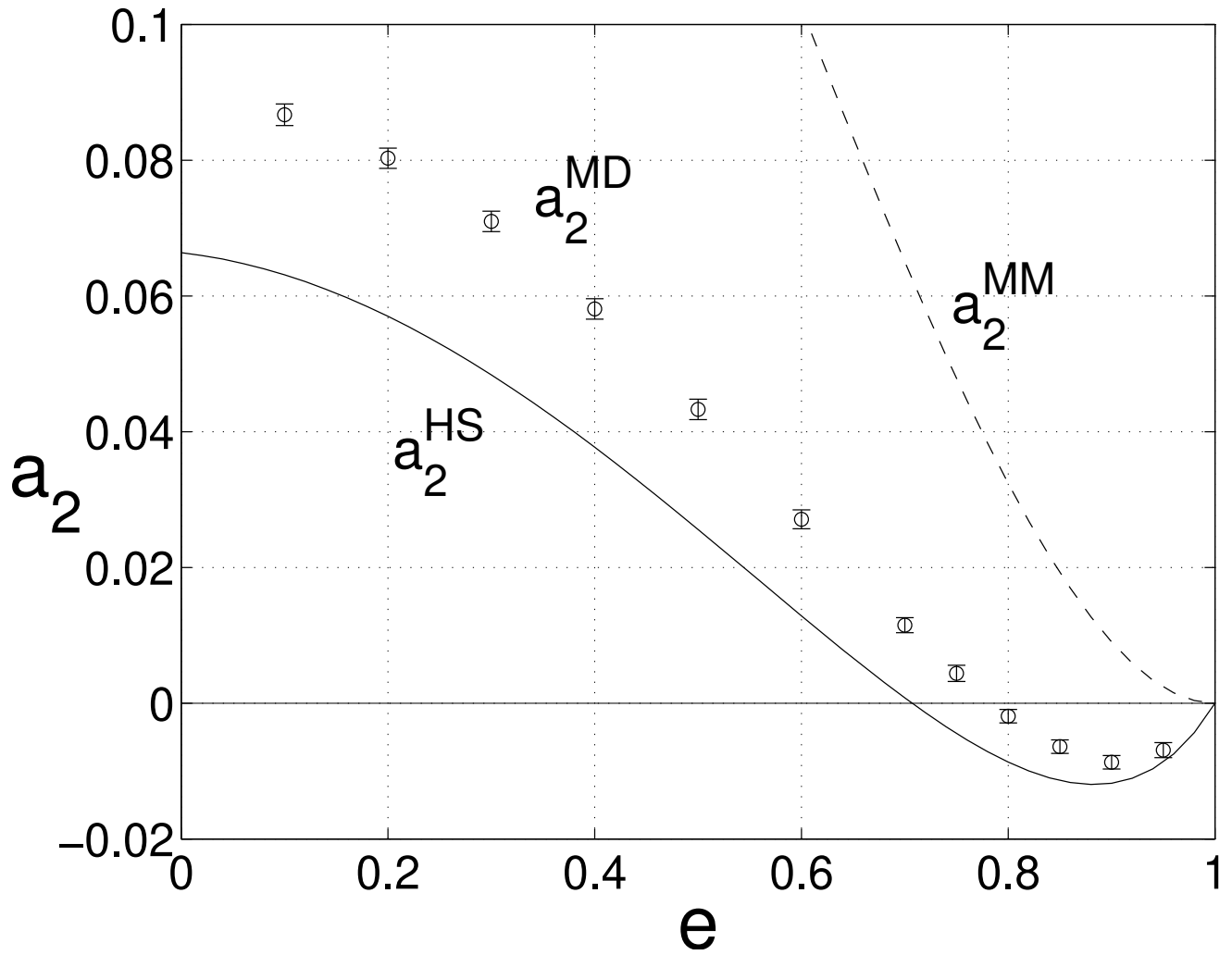


FIG. 4. A comparison of a_2 's obtained from the kinetic theory of the inelastic hard sphere model (solid curve) and the pseudo-Maxwell molecule mode (dashed curve), and that obtained from the MD simulation (open circles). The volume fraction is $5\nu_o$.

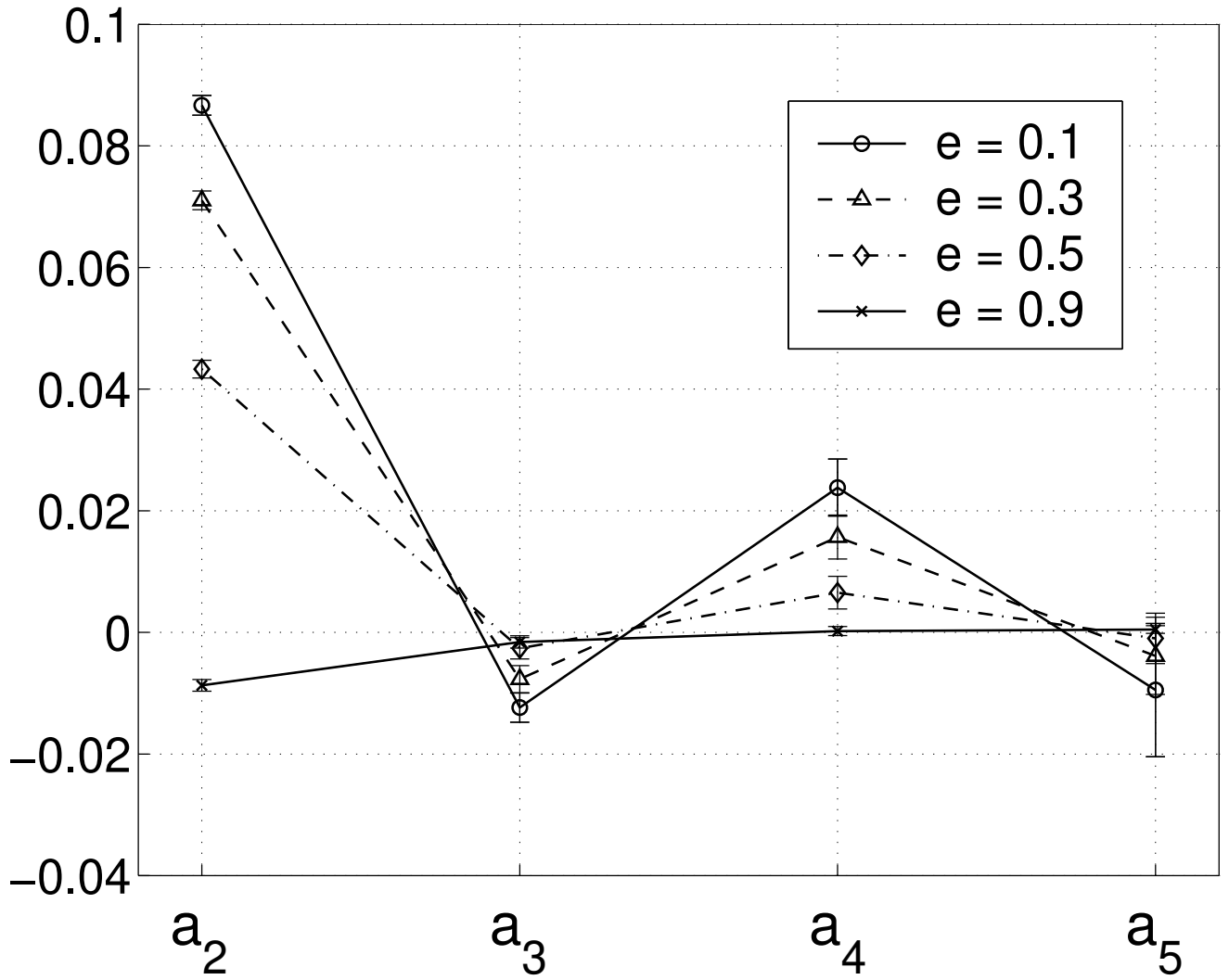


FIG. 5. The first four nonvanishing coefficients of the Sonine polynomial expansion of the simulation results, a_2 , a_3 , a_4 , and a_5 , for four coefficients of restitution. The volume fraction is $5\nu_o$.

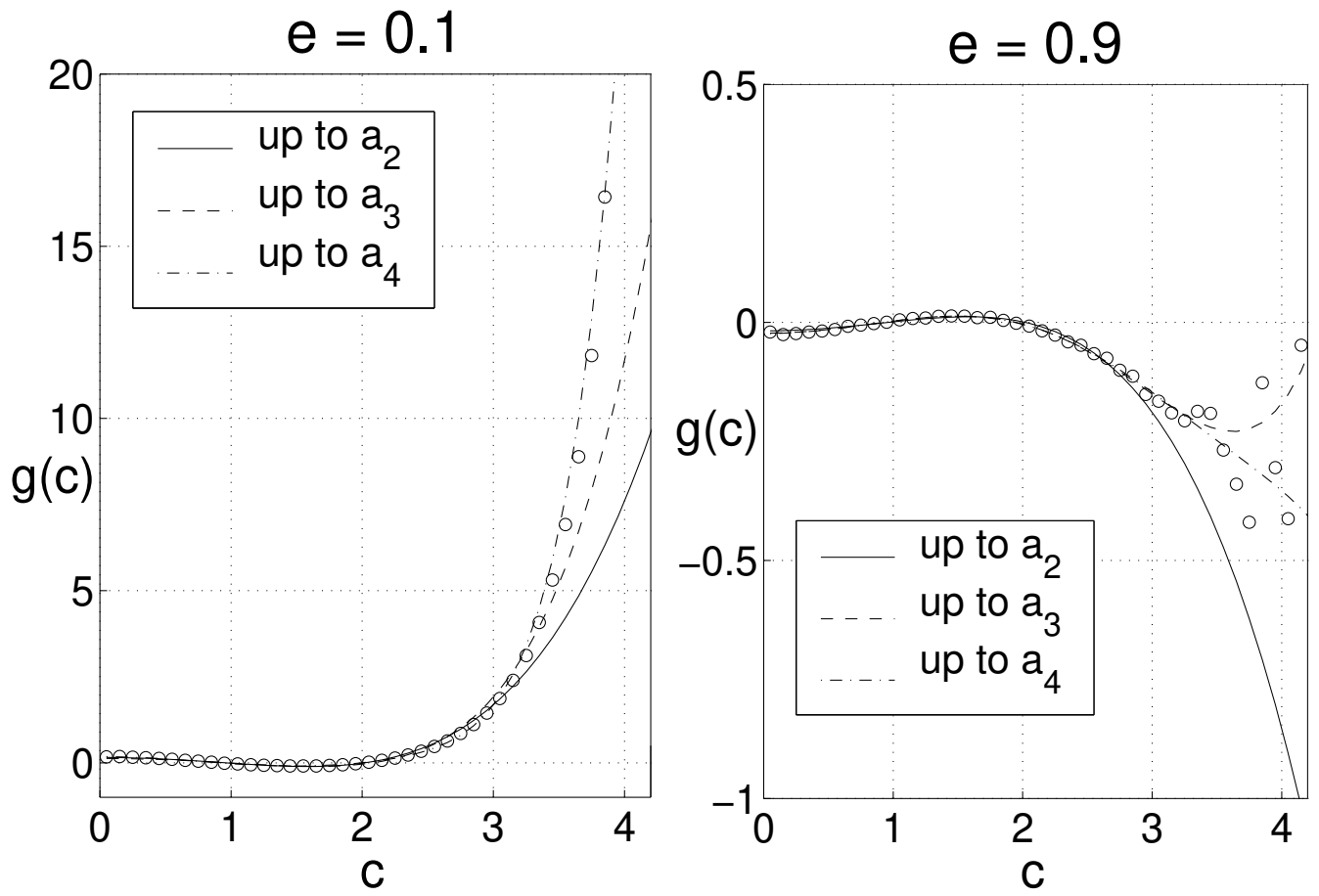


FIG. 6. The normalized deviations from the Maxwell-Boltzmann distribution, $g(c)$, obtained in the simulation (open circles), and the fitted curves using the coefficients of the Sonine polynomial expansion of the simulation results. These are shown for two coefficients of restitution, $e = 0.1$, and $e = 0.9$. The terms are successively added to the expansion up to a_4 . The volume fraction is $5\nu_o$ for both.

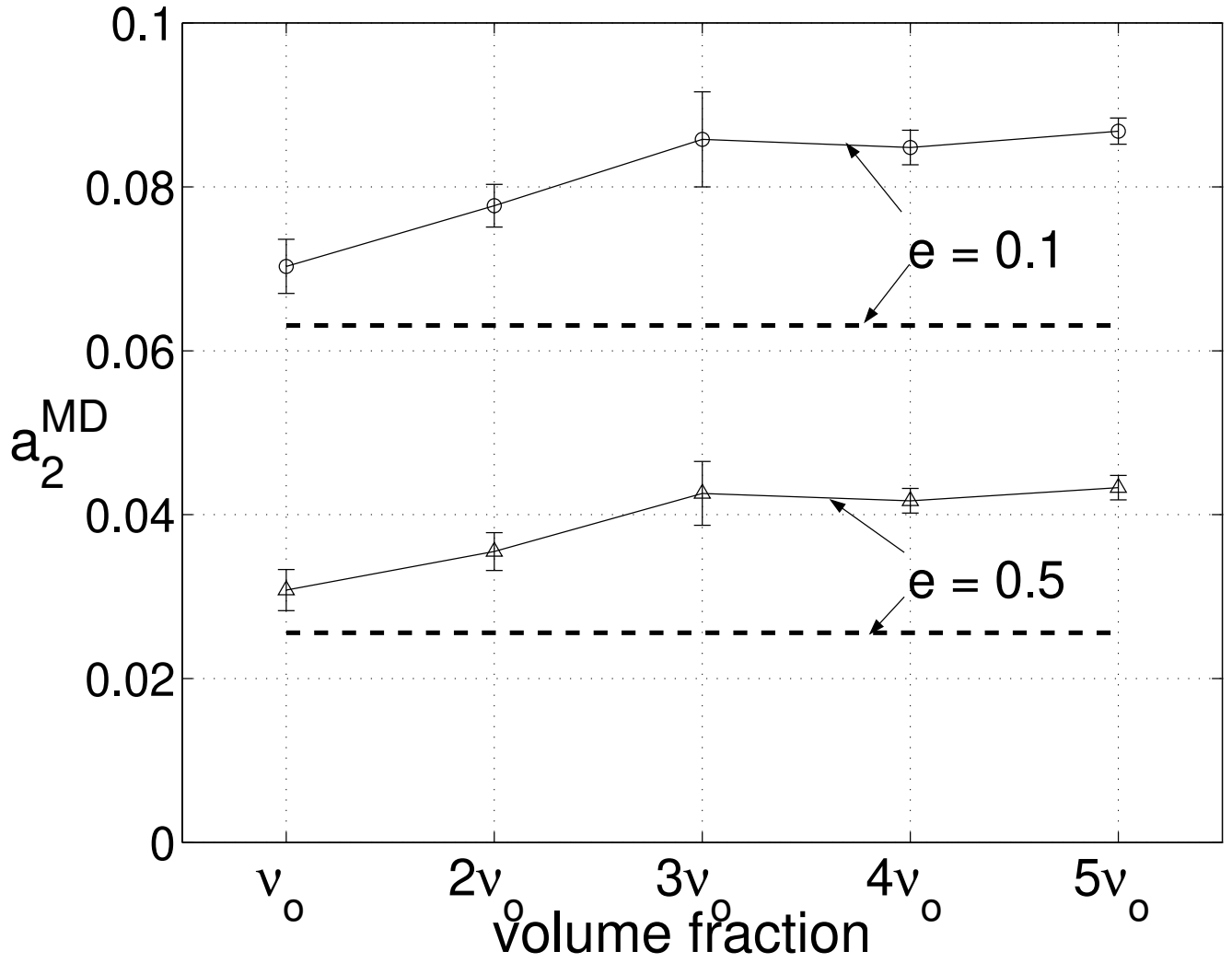


FIG. 7. The values of a_2 obtained in the simulation as a function of density for two coefficients of restitution, $e = 0.1$ and $e = 0.5$. Dashed lines are the predictions of the inelastic hard sphere kinetic theory, which do not depend on the density.

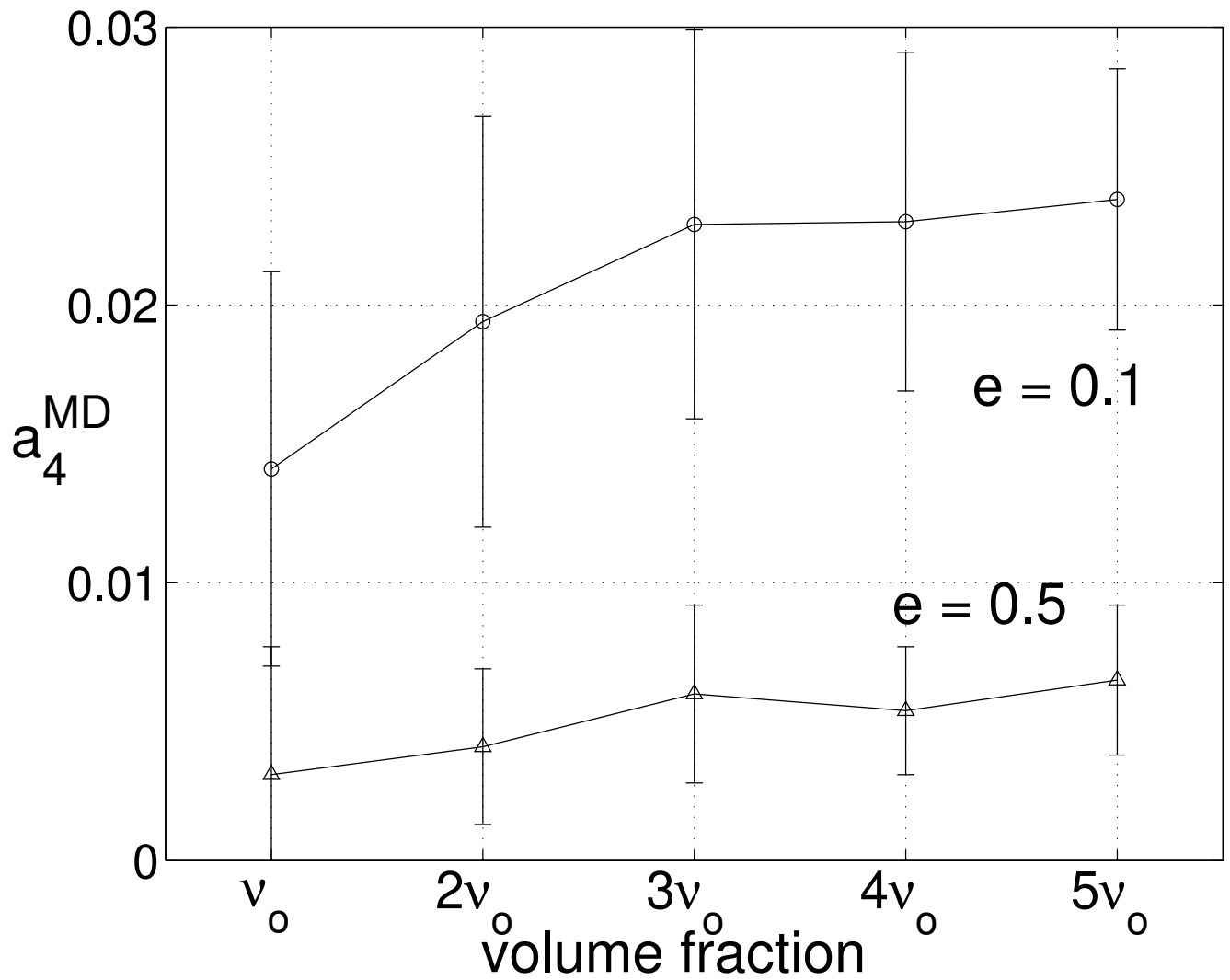


FIG. 8. The density dependence of a_4 for two coefficients of restitution, $e = 0.1$ and $e = 0.5$, obtained in the simulation. Predictions are not shown, because they have not been calculated in the theoretical studies.

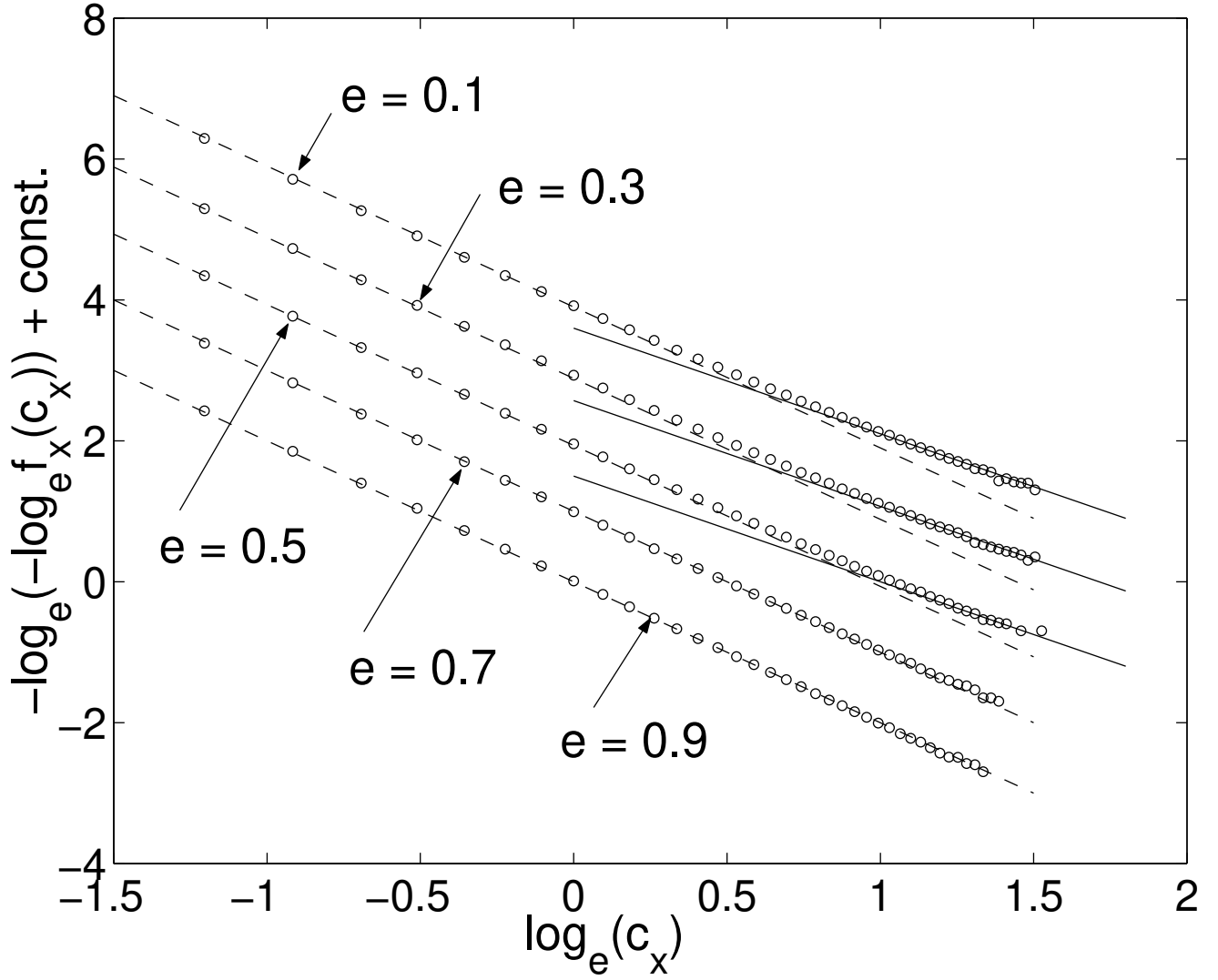


FIG. 9. The velocity distribution functions in x -direction for various coefficients of restitution. The open circles are data obtained from the simulation. The dashed lines are $\sim \exp(-\mathcal{A}c_x^2)$, and the solid lines are $\sim \exp(-\mathcal{A}'c_x^{3/2})$, where \mathcal{A} and \mathcal{A}' are arbitrary constants. For higher inelasticities, a crossover of the exponent is observed. The volume fraction is $5\nu_o$.

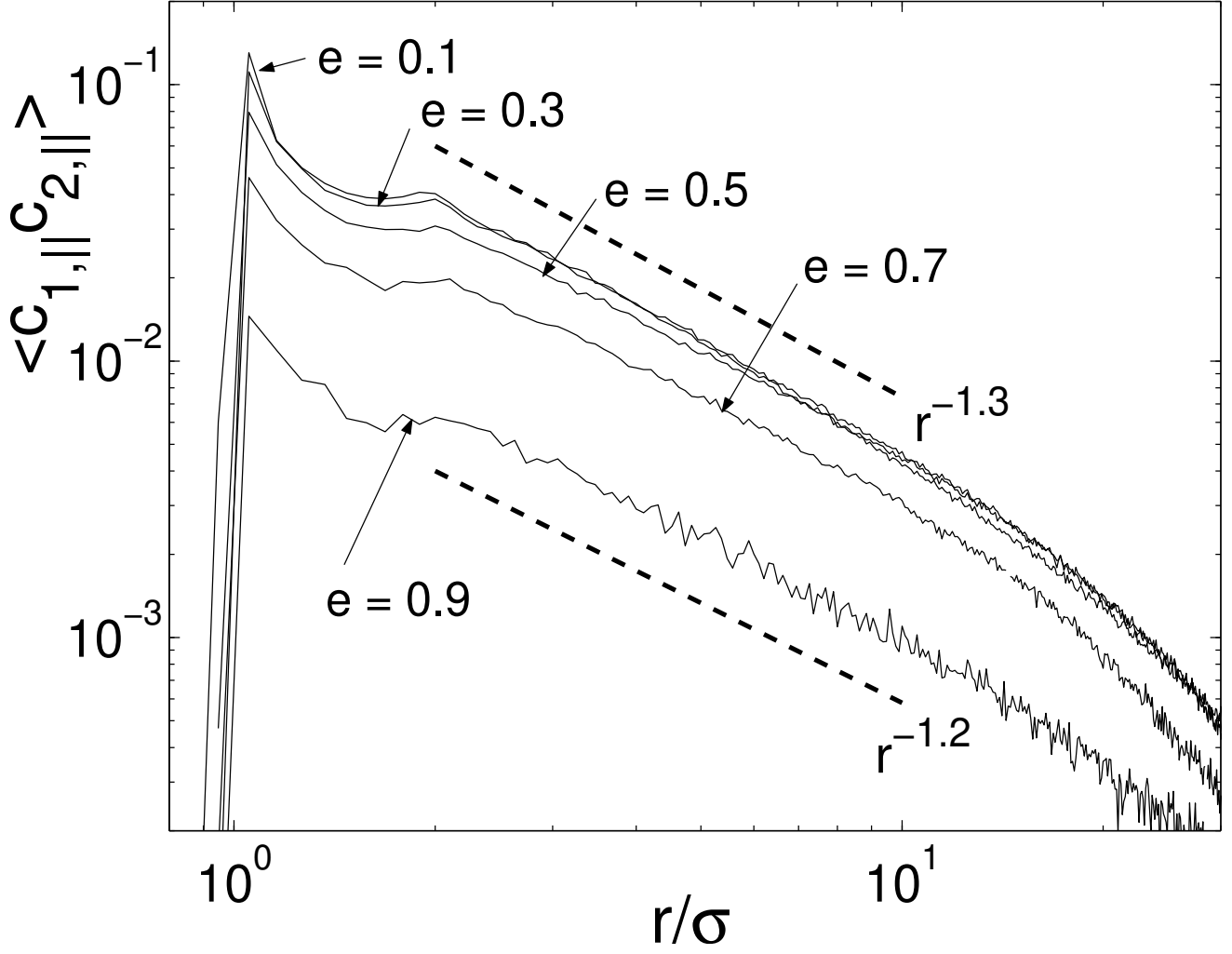


FIG. 10. The parallel velocity correlations for various coefficients of restitution. The volume fraction is $5\nu_o$. Dashed lines are the curves following the power law, which are drawn for comparison. The curves deviate from the power law for $r/\sigma > 20$, because of the finite system size effect. Error bars are not shown for clarity.

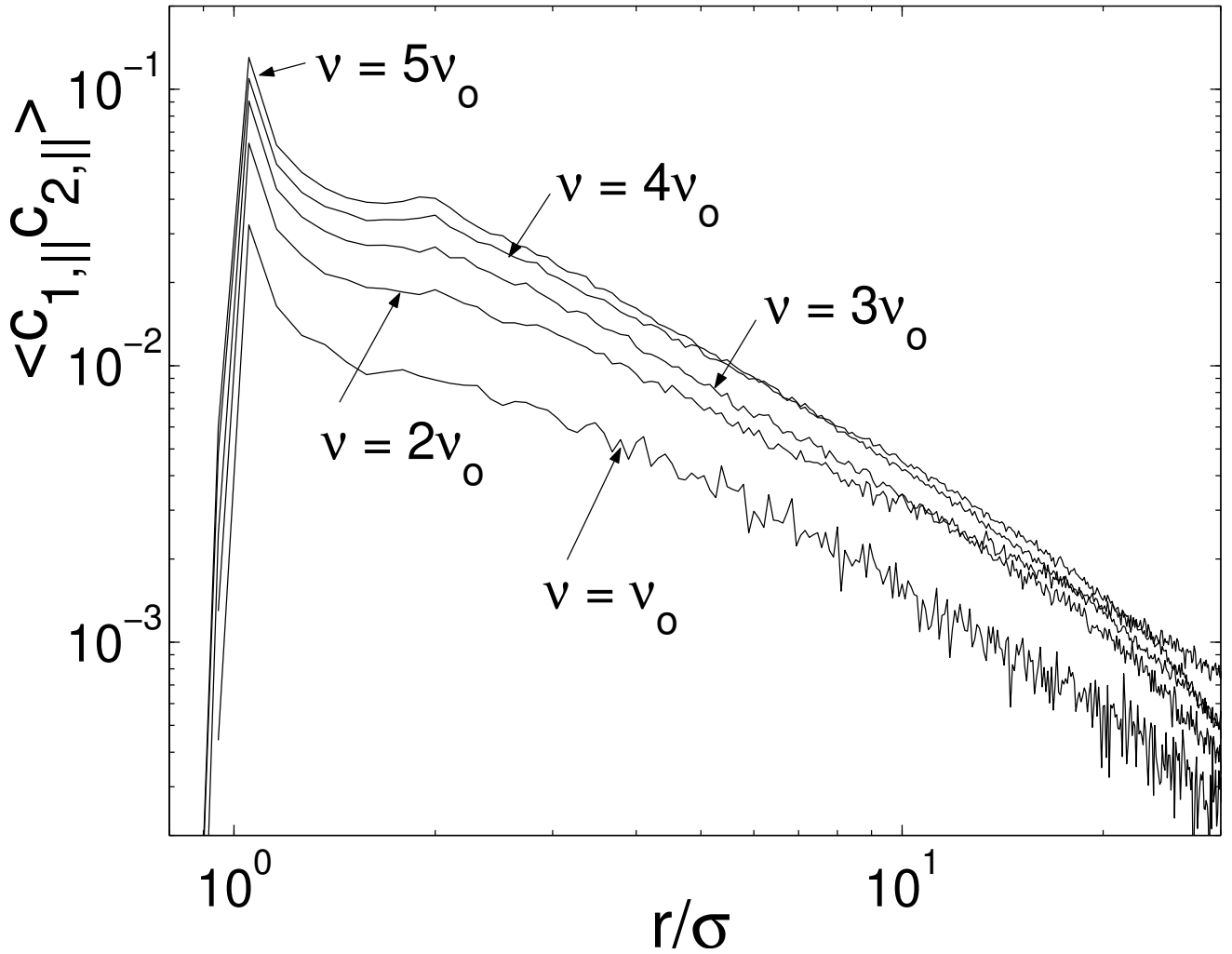


FIG. 11. The parallel velocity correlations for various densities. The coefficient of restitution is 0.1.

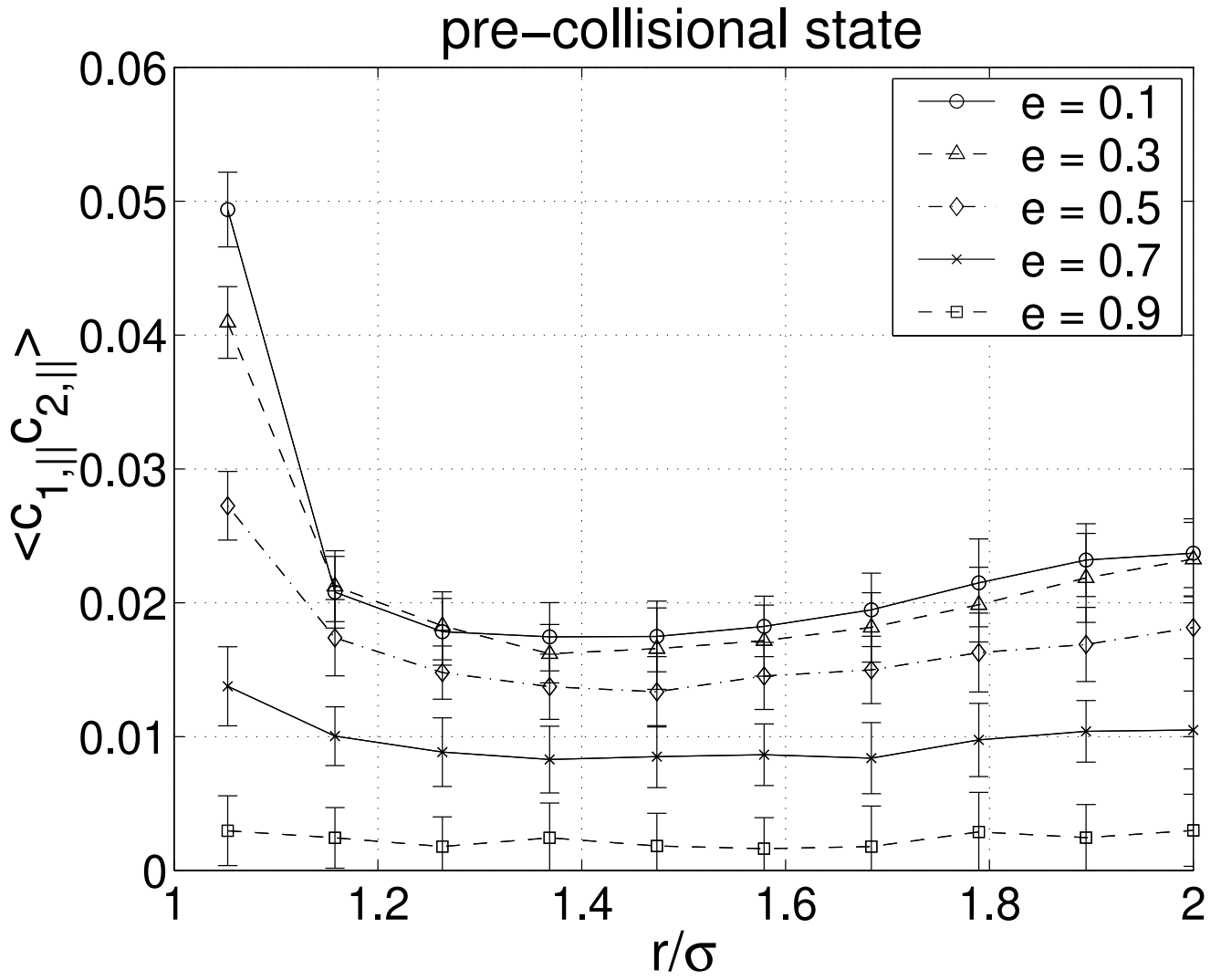


FIG. 12. The short-range pre-collisional parallel velocity correlations for various coefficients of restitution. The volume fraction is $5\nu_0$.

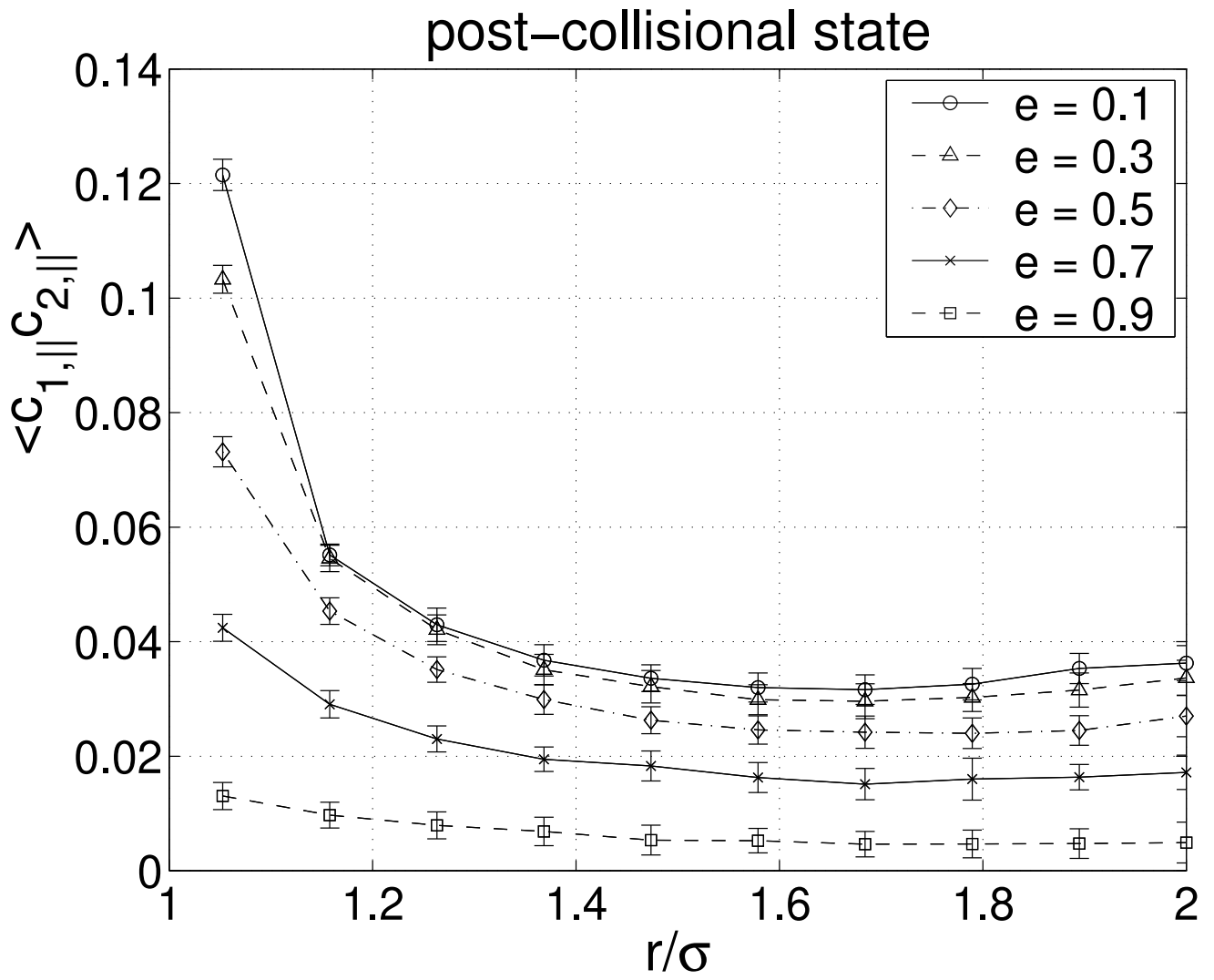


FIG. 13. The short-range post-collisional parallel velocity correlations for various coefficients of restitution. The volume fraction is $5\nu_0$.

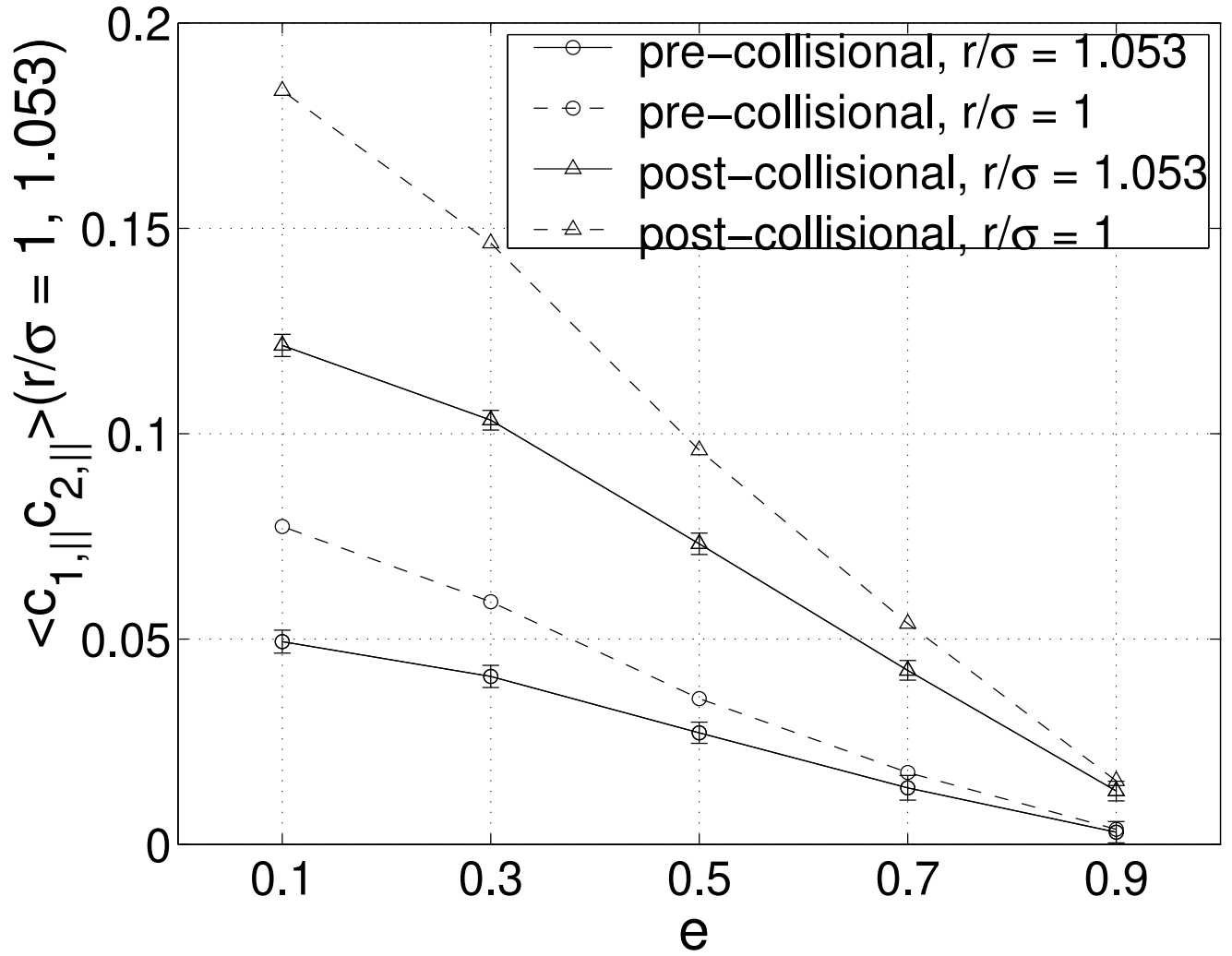


FIG. 14. The pre- and post-collisional parallel velocity correlations at $r/\sigma = 1.053$ (solid lines) and estimated values at contact, $r/\sigma = 1$ (dashed lines), as a function of the coefficient of restitution. The volume fraction is $5\nu_o$. The values at contact are obtained by extrapolating the data in Figure 12 and Figure 13, using fifth order polynomials.

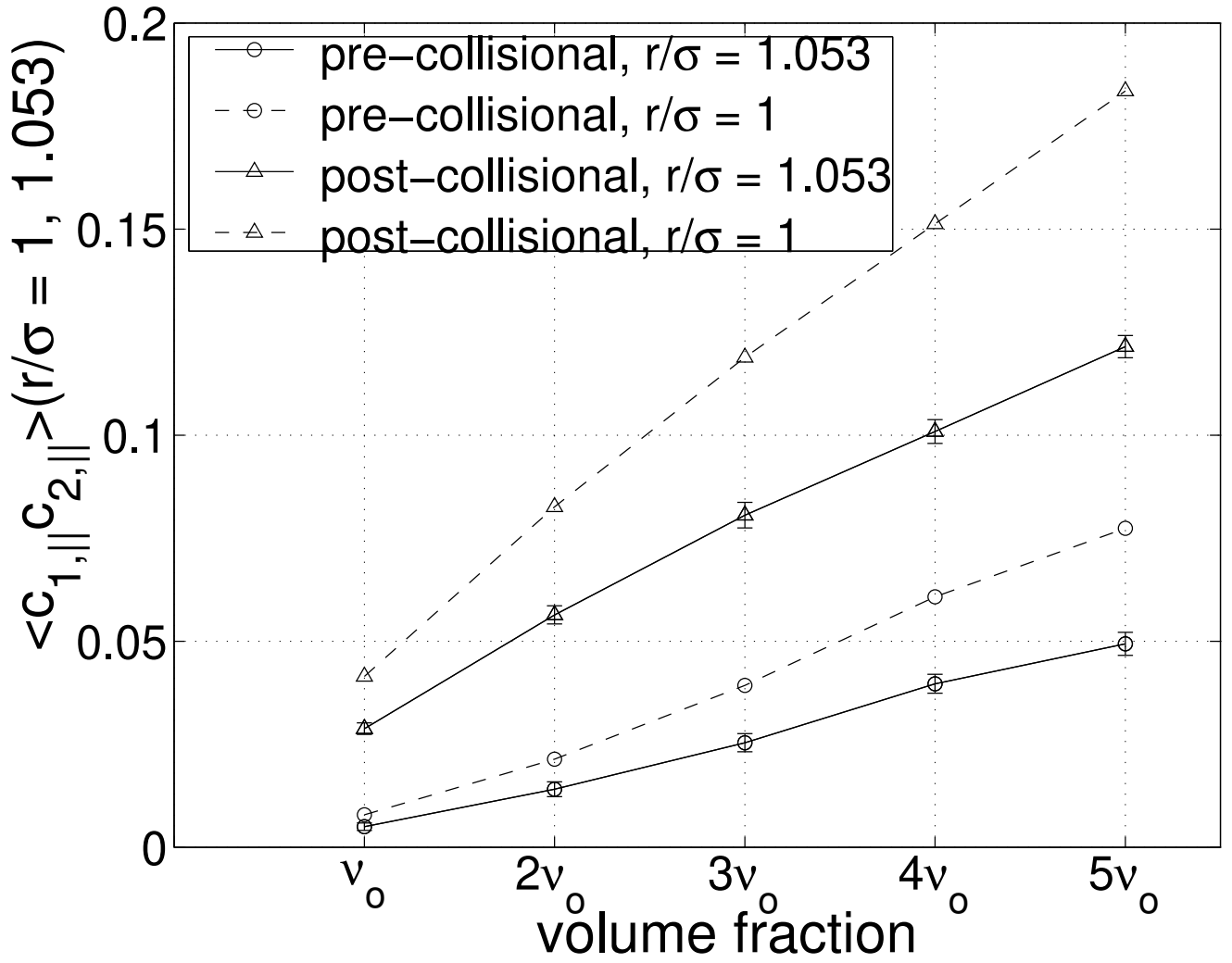


FIG. 15. The pre- and post-collisional parallel velocity correlations at $r/\sigma = 1.053$ (solid lines) and estimated values at contact, $r/\sigma = 1$ (dashed lines), as a function of the density. The coefficient of restitution is 0.1.